Self-calibration of a thinned, backside illuminated charge coupled devices in the soft x-ray region

Yuelin Li,[a] G. D. Tsakiris, and R. Sigel
Max-Planck Institut für Quantenoptik, 85748 Garching, Germany

(Received 8 March 1994; accepted for publication 20 September 1994)

A semiempirical method of calibrating a thinned, backside illuminated charge coupled device (CCD) chip in the soft x-ray region is presented. It is based on determining the thickness of the dead layer self-consistently using the continuum emission from laser produced plasmas. The CCD camera system was coupled to a transmission grating spectrometer and recorded the spectrally resolved continuum emission from laser irradiated tungsten targets. The thickness of the dead layer was then determined by comparing the experimental spectra with the calculated quantum efficiency for a thinned CCD using a simplified model. In this way the CCD chip was semiempirically calibrated. The accuracy of the calibration in the soft x-ray range was assessed by comparing the CCD recorded spectra with those recorded by a spectrometer using the absolutely calibrated Kodak 101 photographic plates and a similar transmission grating. Based on this calibration, the CCD sensitivity is deduced to be about two orders of magnitude higher than that of the Kodak plates in this wavelength range. © *1995 American Institute of Physics.*

I. INTRODUCTION

Recently, charge coupled devices (CCDs), especially the thinned backside illuminated chips,[1,2] have received a great deal of attention because of their potential applications in x-ray imaging,[3,4] soft x-ray spectroscopy of laser produced plasmas,[5,6] and x-ray laser studies.[7,8] They are, together with microchannel plate (MCP) detection systems, becoming the new generation of detectors for soft x-ray (SXR) and vacuum ultraviolet (VUV) radiation replacing the traditional photographic films like Kodak 101.[9–11] There are basically three advantages associated with CCDs over photographic films. The first is the linearity, i.e., they do not need to be calibrated at different exposures for a characteristic response curve. The second is the large dynamic range of the order of $\sim 10^4$, which for film is no larger than 100. Finally, they possess much higher sensitivities. Besides, the film is susceptible to sensitivity variations due to different fabrication and developing conditions, which give rise to irreproducibility. As compared to MCP system (CsI coated), the thinned CCD does not need an additional image readout system and when operated without cooling, it also does not need high vacuum. This makes it more versatile for applications.

In a wide range of applications for the thinned CCDs, it is rather important to know their spectral response, especially for those applications where an absolute measurement is needed. In our group, the calibrated CCD described in the following has been successfully applied to measurements of the gain in x-ray laser experiments. It is also planned to use the CCD to absolutely measure the x-ray laser output energy and the x-ray emission from femtosecond (fs)-laser produced plasmas for x-ray microscopy. Further planned applications include spatially resolved measurements of the emission spectra from colliding laser plasmas and spectrally resolved measurements of the high-order harmonics from fs-laser heated gases and solids. In both cases, quantitative information at different wavelengths is very important for elucidating the physics involved.

The characterization of the spectral response of CCDs is usually done by calibration with standard light source like synchrotron radiation or gas discharge.[3,4,12–17] Because such a standard light source is usually not available, this method cannot be widely applied.

In this paper, we present a simple semiempirical calibration of a thinned backside illuminated chip which consists of determining the dead layer thickness self-consistently using the continuum emission from laser irradiated tungsten slabs. The method does not require an absolutely calibrated standard light source, and it was proved in our experiment to be accurate enough to meet common requirements. The dead layer thickness of the chip is determined by comparing the experimental spectra with the calculated quantum efficiency (QE) from a simplified model. In this way, the CCD is calibrated self-consistently. From comparison with spectra measured with the absolutely calibrated Kodak 101 photographic plate, it is shown that this method works quite accurately in the soft x-ray range. The CCD sensitivity is also deduced to be two orders of magnitude higher than that of the Kodak 101 plates.

II. THINNED CCD AND SIMPLIFIED QE MODEL DESCRIPTION

A common CCD is illuminated from the front side, where the incident light has to cross the whole gate structure and a silicon oxide layer of about thousand angstroms. Because silicon and its oxides are opaque to radiation in the soft x-ray and vacuum ultraviolet range (see Fig. 1), a common CCD is only sensitive to visible light and to hard x-rays. To overcome this difficulty, one uses a thinned CCD in which the substrate is removed and, in addition, is illuminated from the back side. This reduces greatly the absorption of the incident photons before they enter the active region. But dur-

[a]Permanent address: Shanghai Institute of Optics and Fine Mechanics, Academia Sinica, P.O. Box 800-211, Shanghai, 201800, China.

 0034-6748/95/66(1)/80/7/$6.00

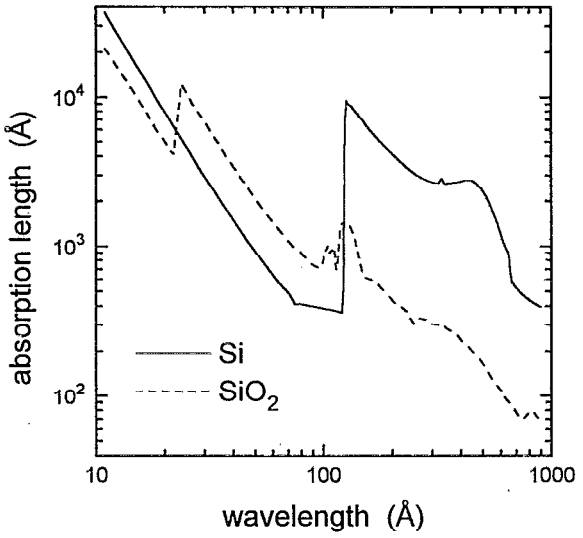

FIG. 1. Absorption coefficients of silicon and silicon dioxide (Ref. 18). The Si L edge is clearly seen.

ing the fabrication of a thinned chip, a layer of silicon oxide (<100 Å) grows unavoidably on the silicon surface. This traps some positive charges at the interface between the oxide layer and the silicon, hence forming a potential driving back the photoelectrons in a region near to the back side. As illustrated in Fig. 2, although some techniques like doping have been developed to reduce the thickness of this region, there still remains a layer in which the electrons diffuse to the back side instead of being collected at the front side. Therefore, these electrons are lost from the counting. This layer is called "dead layer," and behaves phenomenologically like a filter. The absorption coefficients of the silicon and silicon dioxide in Fig. 1 indicate that this dead layer, if of comparable thickness with the oxide layer (assumed to be silicon dioxide in this paper), will dominate the spectral response of the CCD in the soft x-ray range.

From the schematic diagram in Fig. 2, one can derive an approximate expression for the quantum efficiency of a thinned CCD.[12,15,19] The photons reflected at the back-side surface, those going through the CCD chip, and those absorbed by the native oxide layer do not interact with the active region and therefore are unable to create photoelectrons. Thus, the interaction efficiency can be written as

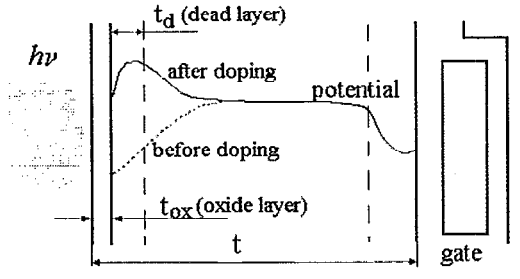

FIG. 2. Schematic diagram showing the structure of a thinned, backside illuminated CCD. In the context of the simple model described in the text, only photons that penetrate the oxide layer and the dead layer are recorded.

$$\eta_{\text{int}}(\lambda)=[1-r(\lambda)]\exp[-\alpha_{\text{ox}}(\lambda)t_{\text{ox}}] \times\{1-\exp[-\alpha(\lambda)t]\},$$

where r, t, t_{ox} are, respectively, the reflectivity at the oxide surface, the thickness of the active region and that of the oxide layer. α and α_{ox} are the related absorption coefficients shown in Fig. 1.[18] The first two terms represent the fraction of photons reaching the active region while the last term is the absorption in the active region. The reflectivity of the surface is negligibly low for the interesting wavelength range and therefore is ignored in the calculation.

The collection efficiency can be expressed in terms of the transmission of the photons through the dead layer, i.e.,

$$\eta_{\text{coll}}(\lambda)=\exp[-\alpha(\lambda)t_d],$$

with t_d the thickness of the dead layer. The diffusion process of the photoelectrons towards the back side of the device that results in their loss is phenomenologically approximated here by the optical absorption of the photons occurring in the dead layer. A more accurate description of the collection efficiency could be obtained by solving the diffusion equation of the photoelectrons produced in the whole CCD active region.[17,20,21]

The quantum efficiency QE is the product of the interaction and collection efficiency, i.e.,

$$\text{QE}(\lambda)=\eta_{\text{int}}(\lambda)\,\eta_{\text{coll}}(\lambda).$$

The quantum yield of the device is therefore

$$\eta(\lambda)=QE(\lambda)\,\frac{h\nu}{3.65}.$$

The 3.65 eV is the average photon energy necessary for creating a charge pair in the silicon in the SXR and VUV range. The simplified model described here gives, generally speaking, satisfactory results for a thinned CCD.[12,15,16,19] More sophisticated models and simulations of the physics in a thinned CCD can be found in Refs. 2,17,20,21. We specially refer to the semiempirical model by Stern *et al.*, which needs more fitting parameters.[17]

In Fig. 3, the calculated QE is obtained by the above model as a function of the wavelength and for various thickness of the dead layer is given. In the calculation the oxide layer was assumed to be an 100-Å-thick SiO_2 layer and the CCD active region is 10 μm thick. Both quantities do not enter very sensitively in the expression for the QE. In contrast, the existence of the dead layer seriously affects the QE in the region between 60–100 Å. Furthermore, one clearly sees the QE jump at silicon L edge (~120 Å). The main effect of varying the thickness of the dead layer is the change of the height of the QE jump at the silicon L edge. The thickness of the oxide layer affects the QE only at wavelengths longer than 200 Å (see Fig. 1).

The sensitive dependence of the QE jump height on the dead layer thickness can be exploited to determine it. Since this is the only unknown sensitive parameter in the expression for the QE (the QE is not sensitive to variation of the CCD thickness of 10%, and the oxide layer is normally not thicker than 100 Å), one has the possibility to calibrate this

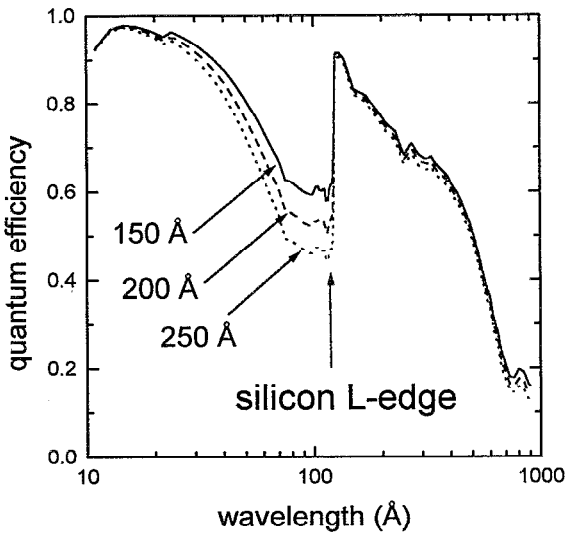

FIG. 3. Calculated quantum efficiency (QE) of a thinned CCD for various dead layer thickness from 150 to 250 Å. The thickness of silicon oxide layer and the CCD were assumed to be 100 Å and 10 μm, respectively. The silicon L edge is clearly seen.

way the device. The quantitative determination of the dead layer thickness is the purpose of the experiment described below.

III. EXPERIMENT AND RESULTS

The experiment was carried out with a frequency-doubled Nd:glass laser system with output energy of up to ~10 J in 3 ns full width at half-maximum (FWHM). The laser beam was normally focused by an $f/4$ lens on the target surface with a focus size ~100 μm. Two spectrometers symmetrically positioned at 45° off the target normal in the same horizontal plane recorded the emitted spectra. Both of the spectrometers were equipped with similar free standing transmission gratings of 1000 lines/mm.[22] For detectors, one of them was coupled to a Photometrics AT200 CCD camera system consisting of a thinned, backside illuminated chip (Tektronics TK512B) working at −40 °C, and the other to absolutely calibrated Kodak 101-05 photographic plates. Tungsten(^{74}W) slabs were used as targets for the production of continuum spectrum. For measuring the high-order efficiencies of the transmission gratings, we used slabs of teflon, which produce a spectrum rich with lines. During the experiment, the target chamber was kept at 10^{-5} Torr, which is not good enough to avoid contamination of the CCD surface (see later discussion).

The CCD camera was not synchronized with the laser pulse, instead the CCD was exposed for 30 s during each shot. After each exposure, a dark current record was obtained and subtracted from the spectrum. The background of the spectrum was quite stable and normally had a standard deviation of 3 counts/pixel. Other parameters provided by the manufacturer of the camera system are listed in Table I. We only used gain of 1 in the experiment.

Figure 4 gives a typical spectrum from tungsten target recorded by the CCD spectrometer. Besides the well known

TABLE I. Parameters of the CCD camera.

Format	512×512 pixel
Pixel size	27 μm×27 μm
Dark current	11.5 e^-/s
Full well capacity	7.46×10^5 e^- (at AD converter limit)
Gain	11.54 e^-/count(1×)
	2.84 e^-/count(4×)
Readout noise	14.5 e^- rms(1×)
	8.5 e^- rms(4×)
Response linearity	0.05%

peaks from the N and O shells, we can also identify the silicon-L absorption edge at about 120 Å. This edge can only be attributed to the existence of the dead layer in the CCD. The quantitative measurement of the intensity jump at this edge enables us to characterize the CCD.

However, due to the higher-order contribution near the edge, the intensity varies with the laser energy because of the changes in spectral features at shorter wavelengths. To obtain the real intensity jump, it is necessary to subtract the high-order contributions from the raw data.

We have chosen a direct way of subtracting the higher orders. This can be done because of the linear response of the CCD to the incident photon energy. The details of this procedure are discussed in the Appendix. After subtracting the higher orders it was found that those spectra taken with different laser energy give a similar intensity jump of about ~40% at the Si L edge, as shown in Fig. 5. The high-order efficiencies of the grating used for the unfolding were measured with the FV II $2p$-$3d$ line at 128 Å from the teflon targets, and were estimated to be 5%, 5%, 3%, 0.7% and 1.6% correspondingly for 2nd, 3rd, 4th, 5th, and 6th order with respect to the first order. In these estimates some error is expected for two reasons. The first is the modulation of the grating efficiency due to the phase effect[22] and the second is that the high-order efficiencies were estimated at peak intensity, which are lower than the integrated efficiency (the line

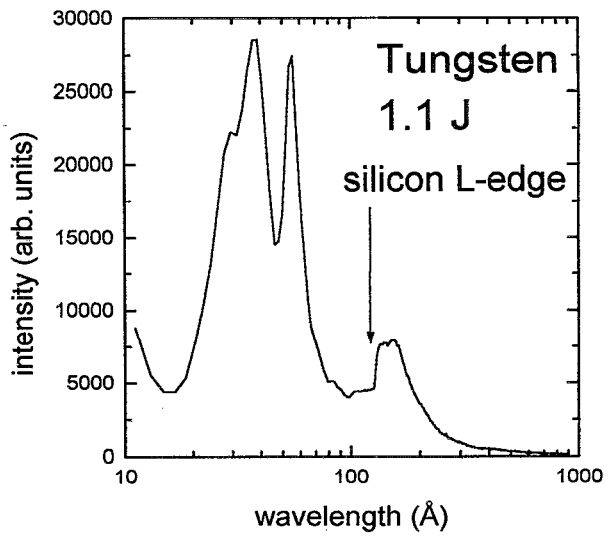

FIG. 4. A typical raw tungsten spectrum measured with CCD. The intensity jump at silicon L edge is due to the existence of the dead layer.

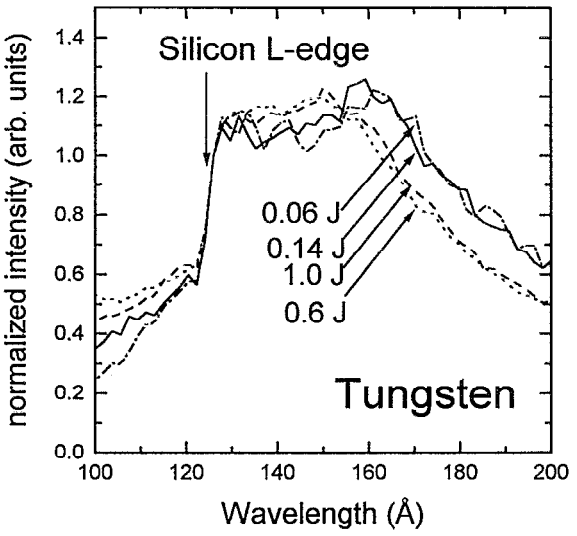

FIG. 5. After subtraction of higher orders, the tungsten spectra taken at the indicated laser intensity show a similar intensity jumping of about 40%±10% at the silicon L edge. In comparison with the calculated quantum efficiency in Fig. 3, the dead layer thickness is deduced to be ~200 Å with an uncertainty of about 20%.

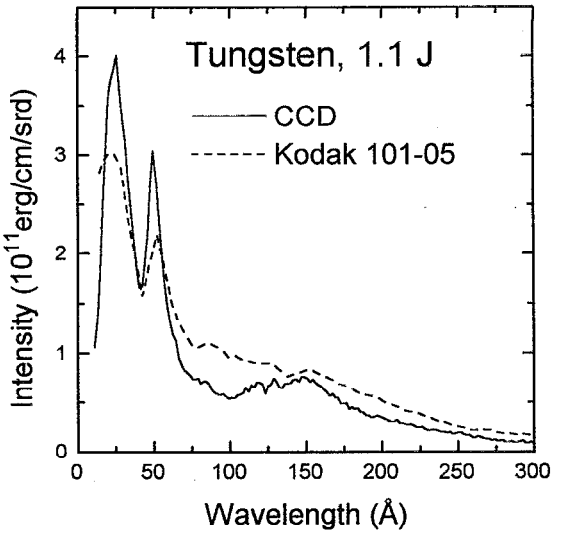

FIG. 6. Comparison of the absolutely unfolded tungsten spectra recorded with CCD and Kodak plates from a single shot. Both spectra were corrected by higher orders, geometry configuration, and detector response. A good quantitative agreement is seen to exist over the whole wavelength scale (note that the intensity scale is linear).

width becomes broader at higher orders) which is required. However, both effects are small as the minor deviation of about 10% observed in the jump indicates.

Comparing the size of the jump in Fig. 5 with the calculated quantum efficiency curves in Fig. 3, one can deduced a dead layer thickness of about 200 Å. The error of 10% in the measurement of the jump leads to a similar uncertainty for the QE, hence to a 20% error for the dead layer thickness. This deduced thickness for the dead layer is of the same order of magnitude with those estimated for different chips by other authors.[3,12,13,16]

After the determination of the dead layer, the calculated QE can be considered as the semiempirical calibration result for the thinned CCD chip. Influence due to condensation of the vacuum oil on the CCD surface (since the CCD works at −40 °C, vapors in the vacuum readily condense on the surface) in this wavelength range is negligible because in our spectrum we cannot see the carbon K edge at 44 Å (the vacuum oil consists mainly of hydrocarbon). More discussion on that can be found in Sec. IV.

By using the absolutely calibrated Kodak 101 photographic plates, the accuracy of the calibration can be tested. We have taken spectra from the same laser shot simultaneously with the CCD and film spectrometers. After the unfolding processes, there is a quantitative good agreement between the spectra from the two detectors. An example of this comparison is shown in Fig. 6, in which the spectra from a single shot recorded simultaneously by the CCD and the Kodak 101-05 photographic plate are shown. Both spectra are corrected for high orders and the spectral response of the detectors. The geometry configuration was also taken into account to obtain the absolute intensity. The first order efficiency of the grating was assumed to be 10% (the method of the data analysis used can be found in Li *et al.*[23] A short description is also given in the Appendix). The CCD response was taken from Fig. 3 with a dead layer thickness of 200 Å, and the calibration data from Henke *et al.*[9] and Kishimoto[10] were used for the Kodak plates. Taking into account the uncertainty involved in the film calibration and that resulting from the development process of the Kodak plates, the two spectra are in good quantitative agreement with each other. The absolute value agrees also with the measurement by Kishimoto[10] when the difference in laser energy is taken into account. This comparison showed that the method we present here for the calibration of the thinned CCD is reasonably accurate in the soft x-ray range.

Based on this calibration, it is of interest to go further and make a comparison of the sensitivity of the CCD with that of the Kodak 101 photographic plates. In Fig. 7, we give the energy density (erg/cm^{-2}) needed to produce the lowest readable signal for both the CCD and the Kodak 101 plates. For the Kodak 101 plates, the lowest reliable density taken from Henke *et al.* and Kishimoto is about 0.2. For the CCD, we assume a lowest readable count to be about 10/pixel, which in our case is well above the noise level of about 3 counts/pixel. As expected, the overall CCD sensitivity is about two orders of magnitude higher than that of the Kodak film.

IV. DISCUSSION

Despite the good agreement in Fig. 6, we notice in the absolutely unfolded spectra a deviation of the CCD from the Kodak data in the wavelength range of 60–100 Å, where the CCD signal is lower. Furthermore, the CCD signal at wavelengths longer than 150 Å exhibits a more rapid decrease (see Fig. 4) than what is expected by taking into account the quantum yield. At wavelength longer than 300 Å, there is almost no signal although the QE predicted by the model is still around 60%. Both phenomena indicate that the model prediction of the QE for the above two wavelength regions is

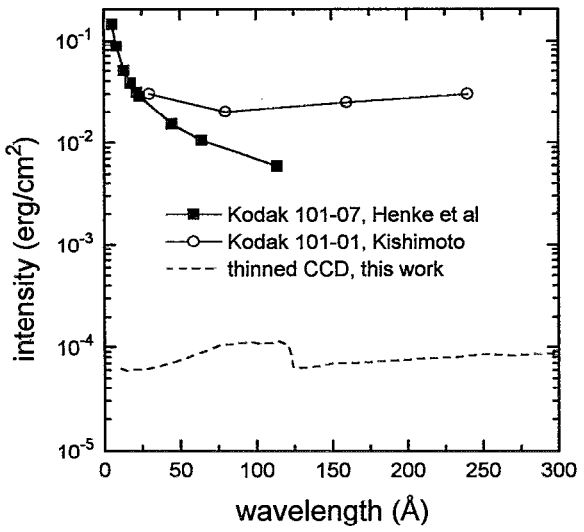

FIG. 7. Comparison of the sensitivity of the CCD and the Kodak 101 photographic plates. We assume that the lowest reliable density for film to be about 0.2 [the data were taken from Henke *et al.* (Ref. 9) and Kishimoto (Ref. 10)]. The lowest readable count for the CCD is assumed to be about 10/pixel, which is well above the background level (~3/pixel for standard deviation). Obviously, the CCD is about two orders of magnitude more sensitive than the Kodak 101 photographic plates.

too high. Noting the difference of optical absorption coefficients of silicon for these two regions (see Fig. 1), one can conclude that the deviations at the short (60–100 Å) and the longer wavelength range (>150 Å) are caused by different mechanisms.

The reason for the short wavelength range is probably the filter approximation for the dead layer, which means that the backwards diffusion of the photoelectrons is only localized in a thin layer. In fact, the probability of backwards diffusion is a function of the position where the photoelectrons are generated, which results in a more complicated expression for the collection efficiency. A model that includes this effect has been proposed by several authors.[17,20,21] In the recent work from Stern *et al.*,[17] an empirical model including two fitting parameters (the backside recombination probability and the implanted region thickness) reproduces the measured QE to a very good accuracy.

For the longer wavelength range, in addition to the above reason, contamination due to impurities in the operating environment is a more important reason. This decrease of QE at long wavelengths caused by contamination has been observed by Hochedez[14] and in the early work of Stern *et al.*,[16] and has been attributed to the hydrocarbons existing in the vacuum chamber. As our vacuum is about 10^{-5} Torr, the contamination may be worse. Although it is possible to include this effect by adding one term describing an effective "carbon filter" in the interaction efficiency, it is still difficult to have an accurate description because the thickness is not constant due to the changing environment and therefore difficult to determine. In our case, since we can not see the carbon K edge at 44 Å, the effective carbon contamination layer is estimated well below 200 Å (this thickness causes 10% jump of the intensity at the K edge and usually cannot be clearly seen) and therefore, it affects the QE only at longer wavelengths range beyond the region we are interested in (the absorption length of graphite carbon at 200 Å is only about half as that at the K edge). Nevertheless, because in laser plasma experiment ultrahigh and clean vacuum is usually not available, special care should be taken to avoid contamination if reproducible data are to be obtained.

It should be indicated that, because of the uncertainties in the fabricating processes of a thinned CCD, the characteristics of the device changes from chip to chip. Therefore, each of the chips should be calibrated separately. Our method appears to be attractive and very practical for that purpose and, in addition, provides a reasonable accuracy in the soft x-ray range.

APPENDIX: METHOD OF UNFOLDING THE RAW SPECTRA

A. Subtraction of higher orders for detectors with linear response

In most of the cases, in the spectra recorded by a transmission grating spectrometer, there exists a lower wavelength cutoff λ_c, below which there is no dispersed spectral component. This cutoff can either come from the transmission grating itself due to the fact that the grating bars become completely transparent to photons with high enough energy and therefore lose the capability of diffraction; or, as is most of the cases, from the source itself. In this case, the spectrum between $\lambda_c - 2\lambda_c$ is free of higher orders. This enables us to remove the higher orders in the whole spectrum starting from λ_c and progressively working up to long wavelength region. When the response of the detector is linear to the incident radiation intensity like in the case of a CCD, the subtraction of the higher orders from the raw spectra can be performed without knowing its spectral response.

For simplicity, we assume a source with (a) a continuum spectrum $[dI_s(\lambda)/d\lambda]$ and (b) having spectral components sharing a similar flat spatial profile with width S. As in our case, if the quantum yield of the detector (the CCD) is $\eta(\lambda)$, the gain is g, and the mth order grating efficiency is $\eta_g^m(\lambda)$, then the detected signal $I'(x)$ by a detection element at a position $x=\lambda L/d$ from the zeroth order is given as the linear superposition of all dispersed orders from different spectral components, i.e.,

$$I'(x)=g\delta\frac{dI_s(\lambda)}{d\lambda}\,\eta(\lambda)\,\eta_g^1(\lambda),\quad \lambda<2\lambda_c, \tag{A1a}$$

$$I'(x)=g\delta\sum_{m=1}^{\infty}\frac{dI_s(\lambda/m)}{d\lambda}\,\eta(\lambda/m)\,\frac{\eta_g^m(\lambda/m)}{m},$$

$$\lambda\geq 2\lambda_c. \tag{A1b}$$

Here δ is the geometry parameter related to the imaging of the source by the slit of spectrometer on the detector, and can be approximated as

$$\delta=\left(\frac{dx}{L+D}\right)^2\left(\frac{L+D}{D}w+\frac{L}{D}S\right)\frac{d}{L},$$

with dx the pixel size of the detection element and L,D,w the detector-grating distance, the grating-target distance, and the slit width of the spectrometer, respectively. d is the grating period.

Starting from the cutoff wavelength, we can evaluate the net signal by taking out the terms of the first order in the summation with the following relations:

$$\frac{dI_s(\lambda)}{d\lambda}\,\eta(\lambda)\,\eta_g^1(\lambda)g\delta=I'(x),\quad \lambda<2\lambda_c,$$

$$\frac{dI_s(\lambda)}{d\lambda}\,\eta(\lambda)\,\eta_g^1(\lambda)g\delta$$

$$=I'(x)-g\delta\sum_{m=2}^{\infty}\frac{dI_s(\lambda/m)}{d\lambda}\,\eta(\lambda/m)\,\frac{\eta_g^m(\lambda/m)}{m},$$

$$\lambda\geqslant 2\lambda_c.$$

Assuming that grating efficiencies are independent of the wavelengths, this becomes

$$\frac{dI_s(\lambda)}{d\lambda}\,\eta(\lambda)=\frac{I'(x)}{g\delta\eta_g^1},\quad \lambda<2\lambda_c, \tag{A2a}$$

$$\frac{dI_s(\lambda)}{d\lambda}\,\eta(\lambda)=\frac{I'(x)}{g\delta\eta_g^1}-\sum_{m=2}^{\infty}\frac{dI_s(\lambda/m)}{d\lambda}$$

$$\times\eta(\lambda/m)\,\frac{\eta_g^m}{m\eta_g^1},\quad \lambda\geqslant 2\lambda_c, \tag{A2b}$$

which contains only the net signal of a single spectral component and is free of the higher-order contributions.

B. Unfolding of film data

For film, the situation is slightly more complex because the optical density changes nonlinearly with the incident intensity. Assuming a known characteristic response curve, this problem has been solved by Li *et al.*[23] Here we apply the results to obtain the formula used in this work. Again assuming a lower cutoff wavelength λ_c, equations similar to Eq. (A1) can be written for the overall optical density D_x' at the position $x=\lambda L/d$ from the zeroth order as

$$D_x'=D_\lambda[J(1,\lambda)],\quad \lambda<2\lambda_c, \tag{A3a}$$

$$D_x'=\sum_{m=1}^{\infty}D_{\lambda/m}[J(m,\lambda)],\quad \lambda\geqslant 2\lambda_c, \tag{A3b}$$

where D_λ is the net optical density produced by a single spectral component of wavelength λ, and

$$J(m,\lambda)=\delta\,\frac{dI_s(\lambda/m)}{d\lambda}\,\frac{\eta_g^m(\lambda/m)}{m}$$

is the intensity of the mth diffraction order from a shorter wavelength component which can be obtained from λ_c to longer wavelength progressively with the known characteristic curve. Therefore, the net density D_λ is

$$D_\lambda\left(\frac{dI_x(\lambda)}{d\lambda}\right)=D_x',\quad \lambda<2\lambda_c, \tag{A4a}$$

$$D_\lambda\left(\frac{dI_s(\lambda)}{d\lambda}\right)=D_x'-\sum_{m=2}^{\infty}D_{\lambda/m}[J(m,\lambda)],\quad \lambda\geqslant 2\lambda_c. \tag{A4b}$$

The characteristic response curves for the Kodak plates were obtained by joining at 45 Å the semiempirical formula of Henke *et al.*,[9] which shows that the optical density is a function of incident photon number, to the data of Kishimoto,[10] which show the density as the function of the incident energy beyond 45 Å, i.e.,

$$D_\lambda=a_1[1-\exp(-b_1\beta_1 I)],$$

where $a_1=1.957$, $b_1=0.3128$ (μm^2). When $\lambda<45$ Å, $\beta_1=1$, and I is the number intensity of the incident photons (μm^{-2}); for $\lambda\geqslant 45$ Å, $\beta_1=(275\text{ eV})^{-1}$, and I is the energy intensity ($eV/\mu m^2$).

ACKNOWLEDGMENTS

The authors are very grateful to A. Böswald, W. Fölsner, and H. Haas for the excellent technical help. One of the authors (Y.L.) was supported by the Alexander von Humboldt Foundation, he would like to thank Dr. S. Witkowski for his hospitality.

[1] J. R. Janesick, T. Elliott, H. H. Marsh, S. Collins, J. K. McCarthy, and M. M. Blouke, Rev. Sci. Instrum. **56**, 796 (1985).
[2] J. Janesick, T. Elliott, S. Collins, T. Daud, D. Compell, A. Dinginzian, and G. Garmire, Proc. SPIE **597**, 364 (1985).
[3] P. Salieres, A. Mens, D. Mazataud, D. Schirmann, and R. Benattar, in *X-Ray Laser 1992*, edited by E. Fill (IOP, Bristol, 1992), p. 367.
[4] A. Mens, R. Benattar, J. L. Bocher, J. M. Koenig, J. P. Le Breton, D. Mazataud, P. Salieres, and D. Schirmann, J. Opt. (Paris) **24**, 129 (1993).
[5] L. Pina, H. Fiedorowicz, M. O. Koshevoi, A. A. Rupasov, B. Rus, A. S. Shikanov, and V. Svoboda, Laser Part. Beams **9**, 579 (1991).
[6] G. M. Zheng, H. Haido, T. Nishikawa, H. Takabe, S. Nakayama, H, Aritome, K. Murai, Y. Kato, M. Nakatsuka, and S. Nakai, J. Appl. Phys. **75**, 1923 (1994).
[7] H. Tsunemi, S. Nomoto, K. Hayashida, E. Miyata, H. Murakami, Y. Kato, G. Yuan, K. Murai, R. Kodama, and H. Haido, Appl. Phys. B **57**, 331 (1993).
[8] J. Nilsen, J. A. Koch, J. H. Scofield, B. J. MacGowan, J. Moreno, and L. B. Da Silva, Phys. Rev. Lett. **70**, 3713 (1993).
[9] B. L. Henke, F. G. Fujiwara, M. A. Tester, C. H. Dittmore, and M. A. Pamler, J. Opt. Soc. Am. **1**, 828 (1984).
[10] T. Kishimoto, Max-Planck Institut für Quantenoptik Report, MPQ 108 (1985).
[11] W. M. Burton, A. T. Hatter, and A. Ridgeley, Appl. Opt. **12**, 1851 (1973).
[12] C. Reverdin, P. Troussel, J. L. Bourgade, F. Le Guern, A. Mens, D. Schirmann, J. M. Dalmasso, D. Gotier, and D. Mazataud, 11th International Workshop on Laser Interaction and Related Plasma Phenomena, Monterey, USA, 1993.
[13] D. Moses, J. F. Hochedez, R. A. Howard, B. Au, D. Wang, and M. M. Blouke, Proc. SPIE **1656**, 526 (1992).
[14] J. F. Hochedez, P. Lemaire, J. P. Delaboudiniere, B. Cougrand, and J. Barba, Proc. SPIE **1070**, 53 (1989).
[15] C. Tassin, Y. Thenoz, R. Lemaitre, and J. Chabbal, Proc. SPIE **1140**, 139 (1989).
[16] R. A. Stern, R. C. Catura, R. Kimble, A. F. Davidsen, M. M. Blouke, R. Hayes, D. M. Walton, and J. L. Culhane, Opt. Eng. **26**, 875 (1987).

[17] R. A. Stern, L. Shing, and M. M. Blouke, Appl. Opt. **33**, 2521 (1994).
[18] E. A. Palik, *Handbook of Optical Constants of Solids* (Academic, London, 1985).
[19] R. A. Stern, R. C. Catura, M. M. Blouke, and M. Winzenread, Proc. SPIE **627**, 583 (1986).
[20] M. M. Blouke, Proc. SPIE **1439**, 136 (1990).
[21] P. Bailey, C. Castelli, M. Cross, P. Essen, A. Holland, F. Jansen, P. Korte, D. Lumb, P. Pool, and P. Verhoeve, Proc. SPIE **1344**, 356 (1990).
[22] K. Eidmann, M. Kühne, P. Müller, and G. D. Tsakiris, J. X-ray Sci. Tech. **2**, 259 (1990).
[23] Y. Li, X. Wang, Z. Xu, S. Chen, and A. Qian, Laser Part. Beams **9**, 787 (1991).